5-8-2014

Kinomic exploration of temozolomide and radiation resistance in Glioblastoma multiforme xenolines

Joshua C. Anderson

Christine W. Duarte

Karim Welaya

Timothy Rohrbach
Richard Bland College of the College of William and Mary, trohrbach@rbc.edu

Markus Bredel

See next page for additional authors

Authors

Joshua C. Anderson, Christine W. Duarte, Karim Welaya, Timothy Rohrbach, Markus Bredel, Eddy S. Yang, Nirmal Choradia, Jaideep V. Thottassery, G. Yancey Gillespie, James A. Bonner, and Christopher D. Willey

Published in final edited form as:
Radiother Oncol. 2014 June ; 111(3): 468–474. doi:10.1016/j.radonc.2014.04.010.

Kinomic exploration of temozolomide and radiation resistance in *Glioblastoma multiforme* xenolines

Joshua C. Anderson[1], **Christine W. Duarte**[2], **Karim Welaya**[1,4], **Timothy D. Rohrbach**[1], **Markus Bredel**[1], **Eddy S. Yang**[1], **Nirmal Choradia**[1], **Jaideep V. Thottassery**[3], **G. Yancey Gillespie**[1], **James A. Bonner**[1], and **Christopher D. Willey**[1,*]

[1]The University of Alabama at Birmingham, AL, USA

[2]Maine Medical Center Research Institute, Portland, ME, USA

[3]Southern Research Institute, Birmingham, USA

[4]University of Alexandria, Alexandria, Egypt

Abstract

Background and Purpose—*Glioblastoma multiforme* (GBM) represents the most common and deadly primary brain malignancy, particularly due to temozolomide (TMZ) and radiation (RT) resistance. To better understand resistance mechanisms, we examined global kinase activity (kinomic profiling) in both treatment sensitive and resistant human GBM patient-derived xenografts (PDX or "xenolines").

Materials and Methods—Thirteen orthotopically-implanted xenolines were examined including 8 with known RT sensitivity/resistance, while 5 TMZ resistant xenolines were generated through serial TMZ treatment *in vivo*. Tumors were harvested, prepared as total protein lysates, and kinomically analyzed on a PamStation®12 high-throughput microarray platform with subsequent upstream kinase prediction and network modeling.

Results—Kinomic profiles indicated elevated tyrosine kinase activity associated with the radiation resistance phenotype, including FAK and FGFR1. Furthermore, network modeling showed VEGFR1/2 and c-Raf hubs could be involved. Analysis of acquired TMZ resistance revealed more kinomic variability among TMZ resistant tumors. Two of the five tumors displayed significantly altered kinase activity in the TMZ resistant xenolines and network modeling indicated PKC, JAK1, PI3K, CDK2, and VEGFR as potential mediators of this resistance.

*Address correspondence to: Christopher D. Willey, MD, PhD, The University of Alabama at Birmingham, Department of Radiation Oncology, Hazelrig-Salter Radiation Oncology Center, Room 2232C, 619 19th Avenue South, Birmingham Alabama, 35249, United States of America, cwilley@uab.edu.

Presented at the 13th International Wolfsberg Meeting 2013

Conflicts of Interest:
No conflicts to disclose

Conclusions—GBM xenolines provide a phenotypic model for GBM drug response and resistance that when paired with kinomic profiling identified targetable pathways to inherent (radiation) or acquired (TMZ) resistance.

Keywords

Glioblastoma; xenolines; kinomics; temozolomide; array profiling

Introduction

GBM is the most deadly malignant brain tumor with an incidence of 14,000 new cases each year in the United States comprising 40–60% of all malignant gliomas [1]. Several genetic and clinical factors affect the prognosis of GBM but generally it has a poor prognosis with a median overall survival of only 14 months with even the most current therapies [2].

GBM is managed with tri-modality therapy including surgery ("maximal safe resection" for the purpose of debulking and pathological sampling), followed by localized radiotherapy (RT) [3], combined with temozolomide (TMZ, an oral alkylating agent) in fit patients [4,5]. Additional chemotherapeutic agents have been tested, and in the case of bevacizumab (a monoclonal antibody that binds to VEGF-A) has shown promise in phase II investigation [6], although it was not shown to be beneficial in a phase III trial [7]. Unfortunately, all available modalities do little to improve outcome in GBM and it is still difficult to achieve local control in many of the patients [8] due to the high incidence of recurrence in these tumors with development of resistance towards these therapies [9]. As such, there has been intense effort devoted to unraveling the molecular biology of this disease in hopes of finding better treatments.

Verhaak et al. identified four molecular subtypes of GBM based on the high content -omic data from The Cancer Genome Atlas (TCGA), including the Classical, Mesenchymal, Proneural and Neural subtypes using the expression of 840 genes representing distinct signaling axes [10]. The *Classical* subtype was characterized by chromosome 7 amplification associated with loss of chromosome 10. Additionally, 97% of the Classical tumors had gene amplification of the EGFR receptor tyrosine kinase. *Mesenchymal* tumors had frequent NF1 focal gene deletions leading to lower protein expression levels of NF1. Overexpression of genes in the TNF superfamily and NFκB pathway were also observed in the *Mesenchymal subtype. Proneural* tumors exhibited 2 major alterations, the first of these being focal amplification and subsequent high levels of PDGFRA gene expression. The second alteration involved point mutations in IDH1. Lastly the *Neural* subtype was characterized by over expression of neuronal markers, such as NEFL, GABRA1, SYT1, and SLC12A5. Even though these subtypesare characterized by alteration in specific kinase signaling pathways, successful translation of these findings into clinical application has not been possible.

Genetic testing has also not been as successful as anticipated in GBM, which is not completely unexpected as genetic or epigenetic alterations may not strongly correlate with altered protein function at the level of therapeutic intervention. Brennan et al. showed this to be the case in GBM for PDGFB where protein levels showed no correlation with mRNA

expression [11]. Similarly, most kinases are regulated through post-translational modification, which may explain the disconnect between the Reverse Phase Protein Array (RPPA) data and the genomic/transcriptomic data seen in the recent TCGA update [12]. There has been interest in trying to profile kinases within brain tumors although some studies rely on mRNA expression for drug candidate target identification [13]. While proteomic and functional proteomic assessments have been made in gliomas [14–16], true measurements of global kinase activity (kinomic profiling) are very few. In one reported study, Sikkema et al. obtained kinomic profiles of pediatric brain tumors including astrocytoma, ependymoma and medulloblastoma using the PamChip® tyrosine kinase profiling system to identify targetable kinase signalling pathways [17], identifying 30 substrates (of the total 144) to be phosphorylated in >90% of the brain tumor lysates with 11 of these substrates showing tumor specificity including CDK2, c-MET, and EGFR-derived substrates.

Multiple mechanisms responsible for RT resistance in GBM have been proposed in the literature including activation of PI3K/Akt signaling axis inhibiting apoptosis and enhancing cell survival rendering the cells resistant to multiple external factors [18–20]. Enhanced DNA repair in CD133 positive cells present at high levels in some tumors also mitigates the effects of RT [21,22]. Other factors include increased levels of EGFR and VEGFR, that can be further modified by hypoxia, leading to activation of pathways promoting proliferation, survival, and angiogenesis in the tumor and stromal component, reducing the response to RT [23–25]. As for TMZ, the most studied mechanism for resistance is the overexpression of MGMT (O6-methylguanine–DNA-methyltransferase), which is a cellular DNA repair protein that removes adducts important in the cytotoxic effect of TMZ [9,26]. Similarly, overexpression of the DNA repair protein ALKBH2 can also mitigate the effects of DNA alkylating agents [27]. While proteomic analysis has been done for chemoresistance in GBM, this has focused more on older chemotherapies such as 1, 3-bis (2-chloroethyl)-1-nitrosourea (BCNU) [28].

The molecular biology of GBM and the underlying mechanisms of treatment-resistance are complex, and it is clear that kinase signaling is important in the progression and treatment resistance of these malignant tumors [29]. Importantly, kinases are highly targetable with kinase inhibitors being one of the largest classes of new drug development in oncology [30]. For this reason, we sought to analyze the kinomic determinants of TMZ and RT sensitivity in the most clinically relevant model of GBM, that of patient-derived xenografts (“xenolines” or “PDX”) [31–33].

Material and Methods

Human Glioma Xenolines

A panel of 13 human high-grade glioma xenolines was maintained by serial passage in athymic nude mice as described previously [31–33]. Some of these xenoline tumors were previously developed by Dr. Jann Sarkaria (Mayo Clinic, Rochester, MN) and provided to the UAB Brain Tumor Animal Model Core facility (directed by Dr. Yancey Gillespie) while some were produced at UAB. Of these, 5 tumors were developed as TMZ-resistant isogenic pairs through serial TMZ treatment of *in vivo* passaged tumors in nude mice, while 8 of

these tumors had previously determined radiation sensitivity profiles [31]. All animal studies were approved by annual review of all methods and procedures by the Institutional Animal Care and Use Committee. To establish intracranial gliomas for characterization, tumors were harvested aseptically, disaggregated with a mixture of enzymes, washed and adjusted to 60×10^6 viable (trypan-blue excluding) cells/mL of serum-free DMEM/F12 medium (MediaTech) containing 5% methylcellulose (400 kDa). Anesthetized athymic nude mice were injected intracranially into the right caudate putamen nucleus with 5 μL of each xenoline cell suspension. Mice were monitored daily and as each developed signs of neurological impairment, the mouse was killed by CO_2 inhalation, perfused with ice-cold phosphate buffered saline and the brain removed. Tumor tissue was surgically excised aseptically. Mean survival post implantation time per each xenoline across biological replicates was recorded.

Kinomic profiling

Each of the tumors in Table 1 was analyzed separately as biological replicates from three individual mice, with each tumor lysed independently and analyzed on a separate array, and on a separate chip. Kinomic profiling of xenoline lysates (lysed in M-Per lysis buffer, Pierce) containing 1:100 Halt's protease and phosphatase inhibitors (Pierce cats. 78420, 78415) was conducted in the UAB Kinome Core (www.kinomecore.com) using the PamStation®12 platform, manufactured by PamGene ('s-Hertogenbosch, Netherlands) similar to our previous work [34]. Briefly after protein quantification (BCA protein determination, Pierce Scientific), total protein lysates were loaded onto the appropriate PamChip® [PTK (tyrosine kinome) or STK (serine/threonine kinome)] in kinase buffer. This platform utilizes a high throughput peptide microarray system analyzing 144 individual tyrosine phosphorylatable peptides, or 144 serine and threonine phosphorylatable peptides imprinted and immobilized in a 3D format to assess kinomic activity in cell or tissue lysates (Figure 1). FITC conjugated antibodies are used for visualization during and after lysates are pumped through the array. Capture of peptide phosphorylation signal is via a computer-controlled charge-coupled device (CCD). Kinomic profiling was analyzed using the Evolve (PamGene) software for initial sample and array processing as well as image capture and BioNavigator (PamGene) for raw data transformation into kinetic (initial velocity) and steady state (postwash) values. Significantly altered peptide lists (phosphosubtrates) were generated for the GBM xenoline lysates based on differences between TMZ resistant and sensitive and again between radioresistant and radiosensitive lysates. These were then uploaded to GeneGo MetaCore (portal.genego.com, Thompson Reuters) for network analysis. Significantly altered peptide lists were cross compared for recurrent upstream kinases as listed per residue in Kinexus kinase predictor (www.phosphonet.ca), and scored according to occurrence with a scoring penalty for being present on both sensitive and resistant lists.

Statistics

Kinomic heatmaps were generated based on the most highly variant (var) phosphosubstrates among the tumors tested using a var >0.65 for radiation resistant set and >0.75 for TMZ set for initial filtration. In addition, phenotypebased (e.g., RT resistant phenotype) kinomic signatures were generated for each phenotype and groups were compared using unpaired,

and paired 2-sided students t-tests where applicable to generate lists of significantly altered peptides. False discovery rates (FDR) using the Benjamini-Hochberg method were calculated for peptides tested. For upstream kinase enrichment results for the radiation resistant phenotype, substrates that were significantly different between resistant and sensitive xenolines were analyzed. We chose to use a more liberal threshold for probes for performing network analysis ($p<0.05$, $FDR<0.5$) as is often done for pathway analysis.[35–37] The top 10 kinases per phosphosubstrate were included, and for probes with multiple phosphorylatable residues, fractional contributions were calculated (i.e. if a probe had 4 residues, it got 0.25 for each residue that had the kinase in the top 10). The proportion of significant substrates that had a particular kinase was compared to the proportion of non-significant substrates containing the same kinase. A Fisher's Exact test was used to determine the significance of upstream kinase scoring.

Kinase Activity Validation

Focused validation of upstream kinases predicted to be active in the resistant tumors included Western blot of phosphotyrosine 397 of FAK, total FAK, phosphotyrosine 402 Pyk2, total Pyk2 (Cell Signaling Technology), Actin (Santa Cruz Biotechnology), as well as the phospho-FGFR1 enzyme-linked immunosorbent assay (Sandwich ELISA cat #12909; Cell Signaling Technology). Western blots were performed as described before.[34,38] ELISA was performed according to the manufacturer's instructions using 10 μg of lysate per sample.

Results

GBM Xenoline Model

In the current study, kinomic activity was measured in GBM xenolines with relevant phenotypic data as listed in Table 1. Patient derived xenolines were used as a model in order to best retain primary tumor characteristics. Kinase activity was measured in 13 GBM xenoline tumors using the PamStation®12 kinomic analysis platform that quantitates kinase activity by measuring the extent to which active kinases within the tumor lysates are capable of phosphorylating specific peptide substrate probes. The kinomic profiles were then compared between phenotypes (e.g. radiation sensitive tumor profiles versus radiation resistant tumor profiles). Significantly altered phosphosubstrates were then mapped to knowledge bases for upstream kinase prediction (Phosphonet) and network modeling (MetaCore) (Experimental model summarized in Figure 1).

Radiation Resistance

Eight xenolines with known radiation sensitivity (based on survival changes following irradiation) [31], were analyzed kinomically with phosphorylation profiles displayed in Figure 2. A variance filter ($var>0.65$) was applied to the combined tyrosine kinome and serine/threonine kinome peptide probe phosphorylation ("phosphosubstrates") intensities in order to identify the phosphosubstrates that best distinguish this group of tumors. Hierarchical clustering of this variance-filtered dataset did not globally separate the tumors (cluster tree on X axis; top) based on radiation resistance (Figure 2A. X axis bottom; R (resistant) or S (sensitive)). We, therefore, used a supervised unpaired t-test comparing

biological replicate phosphosubstrate intensity means between the radiation sensitive and resistant tumors to identify kinomic profiles that significantly differentiated the resistant tumors ($p<0.05$ and $FDR<0.5$). These peptides are listed in Supplemental Table 1 and are depicted as a hierarchical clustered heatmap in Figure 2B. We then applied our upstream kinase algorithm (described in Materials and Methods), to generate a list of kinases likely involved in phosphorylating these residues and identified FAK kinase as the number one kinase involved in radiation resistance (Table 2).

To further analyze the kinomic profiles, we uploaded the Uniprot ID's of the parent gene for each of the significantly altered phosphosubstrates in the radiation resistant tumors and analyzed them using the network modeling knowledge base, MetaCore, and radiation resistance network hubs were mapped to the Direct Interactions Network in Supplemental Figure 1A that also identified FAK1 as the most connected node. Additional nodes of interest were identified using a more stringent FDR cutoff (Supplemental Figure 1B; $FDR<0.3$) through the Shortest Paths Network that included several non-receptor serine/threonine and tyrosine kinases as shown in Supplemental Figure 1C (164 nodes).

A limitation of using phosphosubstrate patterns for identifying upstream kinases is due to the fact that kinases and substrates are "promiscuous;" in other words, each kinase can phosphorylate more than one substrate, and each substrate can be phosphorylated by more than one kinase. For this reason, the upstream kinase prediction algorithm and network modeling approach are tools for enriching for a group of kinases with higher likelihood of having enhanced activity in the model system. Therefore, we performed focused validation of some of the identified kinases. Interestingly, FAK showed the highest activity in the resistant GBM ortho 10 but only limited activity in the remaining tumors (Figure 2C) based on phosphotyrosine 397 FAK/total FAK ratio on Western blotting. Conversely, phospho-FGFR1 ELISA revealed elevated activity in all three resistant xenolines (0.15 v. 0.12, $p=0.0479$).

Temozolomide Resistance

The five isogenic pairs of xenolines selected for TMZ resistance through chronic exposure to TMZ were profiled for kinomic activity. To determine if there was a shared TMZ resistance pattern within the kinome, we used a paired t-test identifying peptides commonly altered in all 5 parental lines as a group relative to all 5 TMZ-resistant daughter lines (See Supplemental Table 2). This did not identify any significantly altered phosphosubstrates after accounting for FDR suggesting no common kinase driven pathway of TMZ resistance was present in these xenolines. This was confirmed through variance filtered ($var>0.75$) hierarchical clustering as shown in Figure 3A with TMZ resistance denoted in the tumor name suffix ("T" for resistant daughter xenoline). As with radiation resistance, the global clustering did not segregate the isogenic pairs as a whole. However, 2 of the 5 pairs (GBM39/39T and GBM59/59T) showed striking differences in kinomic activity in their TMZ derived variants (predominantly increased activity in the TMZ resistant xenolines). Unsurprisingly, these 2 tumors had the highest number of altered and increased phosphosubstrates with very low FDRs (See Supplemental Tables 3 and 4) indicating a strong kinomic component in the TMZ resistance of these tumors. Direct Interaction

Network Mappings of significant phosphosubstrates (FDR<0.1) altered in GBM39T (Figure 3B) and GBM59T (Figure 3C) suggest very different signaling pathways at work in these TMZ resistant tumors. For the remaining xenolines, although direct comparison of individual parent and corresponding TMZ resistant daughter did identify a few phosphosubstrates that were statistically significant (See Supplemental Tables 5–7), most of these changes were considered to be of low confidence due to high FDR values.

Discussion

Patient-derived GBM xenolines provide a powerful model for investigating resistance pathways to clinically relevant therapies, including TMZ and RT. These xenoline tumors retain alterations including EGFRvIII expression and wild-type EGFR amplification that are lost in many cell culture models of GBM grown in plastic [39]. This likely explains the histopathological similarity seen in these xenoline tumors reflecting the invasive and angiogenic nature of the primary tumors. As these tumors are derived from multiple independent patients, the biological scope of activated kinase activity, and potential response to therapeutic agents including TMZ and radiotherapy is more encompassing and representative of patient populations, than that of models based off of immortalized cell lines that have been passaged in serum and cultured on plastic. Given this model, the selection of therapeutic intervention should be as directed as possible to identify relevant targets. Here we used kinomic profiling to look at signal transduction pathways activated in TMZ and radiotherapy resistance, and we identified targetable kinase signaling pathways.

While current classification of GBM into genomically/transcriptomically derived subsets (i.e., molecular subtypes) does offer benefit with prognostic implications,[10] the use of DNA-based markers, such as gene copy number alteration in targets such as VEGFR and EGFR may not predict drug efficacy as most kinases are regulated post-translationally. EGFR is overexpressed in 50% of all gliomas with nearly half of them expressing the EGFRvIII mutant type, this is also true for VEGFR with high incidence of overexpression in glioma [40,41]. Unfortunately this cannot be used to accurately predict drug response, for example, although most GBMs overexpress VEGFR there is high incidence of relapse after treatment with bevacizumab in GBMs especially in the salvage setting [42]. Additionally, at the individual patient level, tumor signaling may not fall into a specific pre-defined category of molecular alterations. Thus, the need to profile signaling directly (e.g., kinomics) on a patient specific basis is paramount to successful drug selection. Indeed, we saw broad differences in signaling alterations both in scope (number) and pathways, within the 5 tumors with engineered TMZ resistance, where only 3 peptides were significantly altered globally, although individual tumors had distinct patterns. This variable kinomic activity seen in TMZ resistance is in stark contrast to the inherent radiation sensitivity profiles that did seem to suggest a more common kinomic pattern of resistance. Nevertheless, our focused validation of potential upstream kinases did show heterogeneity, particularly for FAK, though elevated FGFR1 activity was more uniform in the resistant tumors. Some of the key players identified in our network analysis have been garnering attention in the glioma biology field. FGFR has been implicated in carcinogenesis for a variety of tumors [43], but recent work has identified recurrent somatic alterations in low grade pilocytic astrocytomas [44] and transforming fusions of FGFR1 in GBM [45]. FAK signaling plays a

role in proliferation and migration in GBM [46], and JNK, which is a member of the mitogen-activated protein kinase superfamily, has been implicated in many processes in GBM. Specifically, JNK is associated with the so called “stemness” of the glioma cells (i.e., maintenance of the stem cell properties through maintenance of self renewal of these cells [47]). Targeting of JNK 1 and JNK 2 significantly reduced the ability of new sphere formation in glioma cell lines and it also reduced colony-forming ability. Furthermore, it has been hypothesized that JNK is involved in glioma cell migration through the promotion of interactions between insulin-like growth factor binding protein 2 (IGFBP2) and α5 integrin [48]. Potentially, targeting these pathways prior to radiotherapy could enhance radio-effectiveness, and prognostically could be used to predict poor response. Given the nature of these molecules and pathways identified herein and their role in the progression, proliferation, migration and angiogenesis of GBM and other malignancies, this is not completely surprising.

Validation of these activated pathways in the context of targeted therapeutics is possible with this type of kinomics profiling. Versele *et al.* were able to generate a kinomic response predictor for a multi-targeted tyrosine kinase small molecule inhibitor by using kinomic profiles generated from phenotype-classified (inhibitor sensitive v. resistant) cancer cell lines. Specifically, they took lysates from 27 cancer cell lines and treated them (*ex vivo*) with the small molecule inhibitor just prior to kinomic profiling. The phosphosubstrates that differed between responders and non-responders generated a predictor for drug response in both *in vitro* and *in vivo* xenograft studies [49]. The potential to directly interrogate tissue specimens against potential kinase targeted therapeutics using the platform technology described here is attractive because it requires only small amounts of material (<10μg total protein). A potential therapeutic selection strategy might be: 1) Basal profiling to identify kinase targets, as we have done here; 2) Select a subset of likely kinase inhibitors based off of the basal profile; 3) Validate target-hit through *ex vivo* testing of the kinase inhibitor against the original biopsy specimen that can be performed in a short timeframe (within a few hours). This approach can be first tested using patient-derived xenolines as a biologically relevant or “proband” model of GBM where molecular profiling information can be more easily coupled with tumor phenotype characterization. Specifically, we believe that querying tumors at the level of planned intervention (e.g., kinase inhibition) should lead to the most informed clinical decisions. Likely, a combination of this kinomic data and relevant genomic, proteomic, histologic, and clinical data offers the best systems biology based approach to treating a complex disease such as GBM.

Supplementary Material

Refer to Web version on PubMed Central for supplementary material.

Acknowledgments

This project has been funded in whole or in part with Federal Funds from the National Cancer Institute, National Institutes of Health, under Contract No. HHSN261200800001E. The content of this publication does not necessarily reflect the views or policies of the Department of Health and Human Services, nor does mention of trade names, commercial products, or organizations imply endorsement by the U.S. Government. We also acknowledge NCI grant P20 CA151129 (GYG), S08-221ST T04, and the National Brain Tumor Society Mary Catherine Calisto Systems Biology grant.

References

1. Wen PY, Kesari S. Malignant gliomas in adults. N Engl J Med. 2008; 359:492–507. [PubMed: 18669428]
2. Thumma SR, Fairbanks RK, Lamoreaux WT, et al. Effect of pretreatment clinical factors on overall survival in glioblastoma multiforme: a Surveillance Epidemiology and End Results (SEER) population analysis. World journal of surgical oncology. 2012; 10:75. [PubMed: 22553975]
3. Laperriere N, Zuraw L, Cairncross G. Radiotherapy for newly diagnosed malignant glioma in adults: a systematic review. Radiother Oncol. 2002; 64:259–273. [PubMed: 12242114]
4. Stupp R, Mason WP, van den Bent MJ, et al. Radiotherapy plus concomitant and adjuvant temozolomide for glioblastoma. N Engl J Med. 2005; 352:987–996. [PubMed: 15758009]
5. Stupp R, Hegi ME, Mason WP, et al. Effects of radiotherapy with concomitant and adjuvant temozolomide versus radiotherapy alone on survival in glioblastoma in a randomised phase III study: 5-year analysis of the EORTC-NCIC trial. Lancet Oncol. 2009; 10:459–466. [PubMed: 19269895]
6. Lai A, Tran A, Nghiemphu PL, et al. Phase II study of bevacizumab plus temozolomide during and after radiation therapy for patients with newly diagnosed glioblastoma multiforme. J Clin Oncol. 2011; 29:142–148. [PubMed: 21135282]
7. Gilbert MR, Dignam JJ, Armstrong TS, et al. A randomized trial of bevacizumab for newly diagnosed glioblastoma. N Engl J Med. 2014; 370:699–708. [PubMed: 24552317]
8. Omuro AM, Faivre S, Raymond E. Lessons learned in the development of targeted therapy for malignant gliomas. Mol Cancer Ther. 2007; 6:1909–1919. [PubMed: 17620423]
9. Sze CI, Su WP, Chiang MF, Lu CY, Chen YA, Chang NS. Assessing current therapeutic approaches to decode potential resistance mechanisms in glioblastomas. Frontiers in oncology. 2013; 3:59. [PubMed: 23516171]
10. Verhaak RG, Hoadley KA, Purdom E, et al. Integrated genomic analysis identifies clinically relevant subtypes of glioblastoma characterized by abnormalities in PDGFRA, IDH1, EGFR, and NF1. Cancer Cell. 2010; 17:98–110. [PubMed: 20129251]
11. Brennan C, Momota H, Hambardzumyan D, et al. Glioblastoma subclasses can be defined by activity among signal transduction pathways and associated genomic alterations. PLoS One. 2009; 4:e7752. [PubMed: 19915670]
12. Brennan CW, Verhaak RG, McKenna A, et al. The somatic genomic landscape of glioblastoma. Cell. 2013; 155:462–477. [PubMed: 24120142]
13. Grzmil M, Morin P Jr, Lino MM, et al. MAP kinase-interacting kinase 1 regulates SMAD2-dependent TGF-beta signaling pathway in human glioblastoma. Cancer Res. 2011; 71:2392–2402. [PubMed: 21406405]
14. Du J, Bernasconi P, Clauser KR, et al. Bead-based profiling of tyrosine kinase phosphorylation identifies SRC as a potential target for glioblastoma therapy. Nat Biotechnol. 2009; 27:77–83. [PubMed: 19098899]
15. Kozuka-Hata H, Nasu-Nishimura Y, Koyama-Nasu R, et al. Phosphoproteome of human glioblastoma initiating cells reveals novel signaling regulators encoded by the transcriptome. PLoS One. 2012; 7:e43398. [PubMed: 22912867]
16. Kumar DM, Patil V, Ramachandran B, Nila MV, Dharmalingam K, Somasundaram K. Temozolomide modulated glioma proteome: Role of Interleukin-1 receptor associated kinase-4 (IRAK4) in chemosensitivity. Proteomics. 2013
17. Sikkema, AH.; Diks, SH.; den Dunnen, WF., et al. Cancer Res. Vol. 69. United States; 2009. Kinome profiling in pediatric brain tumors as a new approach for target discovery; p. 5987-5995.
18. Li HF, Kim JS, Waldman T. Radiation-induced Akt activation modulates radioresistance in human glioblastoma cells. Radiat Oncol. 2009; 4:43. [PubMed: 19828040]
19. Chautard E, Loubeau G, Tchirkov A, et al. Akt signaling pathway: a target for radiosensitizing human malignant glioma. Neuro Oncol. 2010; 12:434–443. [PubMed: 20406894]
20. de la Pena L, Burgan WE, Carter DJ, et al. Inhibition of Akt by the alkylphospholipid perifosine does not enhance the radiosensitivity of human glioma cells. Mol Cancer Ther. 2006; 5:1504–1510. [PubMed: 16818509]

21. Tamura K, Aoyagi M, Wakimoto H, et al. Accumulation of CD133-positive glioma cells after high-dose irradiation by Gamma Knife surgery plus external beam radiation. J Neurosurg. 2010; 113:310–318. [PubMed: 20205512]
22. Zeppernick F, Ahmadi R, Campos B, et al. Stem cell marker CD133 affects clinical outcome in glioma patients. Clin Cancer Res. 2008; 14:123–129. [PubMed: 18172261]
23. Karar J, Maity A. Modulating the tumor microenvironment to increase radiation responsiveness. Cancer Biol Ther. 2009; 8:1994–2001. [PubMed: 19823031]
24. Said HM, Hagemann C, Staab A, et al. Expression patterns of the hypoxia-related genes osteopontin, CA9, erythropoietin, VEGF and HIF- 1alpha in human glioma in vitro and in vivo. Radiother Oncol. 2007; 83:398–405. [PubMed: 17524506]
25. Lammering G, Valerie K, Lin PS, Hewit TH, Schmidt-Ullrich RK. Radiation-induced activation of a common variant of EGFR confers enhanced radioresistance. Radiother Oncol. 2004; 72:267–273. [PubMed: 15450724]
26. Hegi ME, Liu L, Herman JG, et al. Correlation of O6-methylguanine methyltransferase (MGMT) promoter methylation with clinical outcomes in glioblastoma and clinical strategies to modulate MGMT activity. J Clin Oncol. 2008; 26:4189–4199. [PubMed: 18757334]
27. Johannessen TC, Prestegarden L, Grudic A, Hegi ME, Tysnes BB, Bjerkvig R. The DNA repair protein ALKBH2 mediates temozolomide resistance in human glioblastoma cells. Neuro Oncol. 2013; 15:269–278. [PubMed: 23258843]
28. Suk K. Proteomic analysis of glioma chemoresistance. Current neuropharmacology. 2012; 10:72–79. [PubMed: 22942880]
29. Blume-Jensen P, Hunter T. Oncogenic kinase signalling. Nature. 2001; 411:355–365. [PubMed: 11357143]
30. Zhang J, Yang PL, Gray NS. Targeting cancer with small molecule kinase inhibitors. Nat Rev Cancer. 2009; 9:28–39. [PubMed: 19104514]
31. Kitange GJ, Mladek AC, Carlson BL, et al. Inhibition of histone deacetylation potentiates the evolution of acquired temozolomide resistance linked to MGMT upregulation in glioblastoma xenografts. Clin Cancer Res. 2012; 18:4070–4079. [PubMed: 22675172]
32. Agnihotri S, Gajadhar AS, Ternamian C, et al. Alkylpurine-DNA-N-glycosylase confers resistance to temozolomide in xenograft models of glioblastoma multiforme and is associated with poor survival in patients. J Clin Invest. 2012; 122:253–266. [PubMed: 22156195]
33. Oliva CR, Nozell SE, Diers A, et al. Acquisition of temozolomide chemoresistance in gliomas leads to remodeling of mitochondrial electron transport chain. J Biol Chem. 2010; 285:39759–39767. [PubMed: 20870728]
34. Jarboe JS, Jaboin JJ, Anderson JC, et al. Kinomic profiling approach identifies Trk as a novel radiation modulator. Radiother Oncol. 2012; 103:380–387. [PubMed: 22561027]
35. Gold DL, Miecznikowski JC, Liu S. Error control variability in pathway-based microarray analysis. Bioinformatics. 2009; 25:2216–2221. [PubMed: 19561020]
36. Haralambieva IH, Oberg AL, Ovsyannikova IG, et al. Genome-wide characterization of transcriptional patterns in high and low antibody responders to rubella vaccination. PLoS One. 2013; 8:e62149. [PubMed: 23658707]
37. Umicevic Mirkov M, Cui J, Vermeulen SH, et al. Genome-wide association analysis of anti-TNF drug response in patients with rheumatoid arthritis. Annals of the rheumatic diseases. 2013; 72:1375–1381. [PubMed: 23233654]
38. Jarboe JS, Anderson JC, Duarte CW, et al. MARCKS regulates growth and radiation sensitivity and is a novel prognostic factor for glioma. Clin Cancer Res. 2012; 18:3030–3041. [PubMed: 22619307]
39. Sarkaria JN, Carlson BL, Schroeder MA, et al. Use of an orthotopic xenograft model for assessing the effect of epidermal growth factor receptor amplification on glioblastoma radiation response. Clin Cancer Res. 2006; 12:2264–2271. [PubMed: 16609043]
40. Grzmil M, Hemmings BA. Deregulated signalling networks in human brain tumours. Biochim Biophys Acta. 2010; 1804:476–483. [PubMed: 19879382]
41. Perry J, Okamoto M, Guiou M, Shirai K, Errett A, Chakravarti A. Novel therapies in glioblastoma. Neurology research international. 2012; 2012:428565. [PubMed: 22530121]

42. Chamberlain, MC.; Lassman, AB.; Iwamoto, FM. Neurology. Vol. 74. United States; 2010. Patterns of relapse and prognosis after bevacizumab failure in recurrent glioblastoma; p. 1239-1241.

43. Ahmad I, Iwata T, Leung HY. Mechanisms of FGFR-mediated carcinogenesis. Biochim Biophys Acta. 2012; 1823:850–860. [PubMed: 22273505]

44. Jones DT, Hutter B, Jager N, et al. Recurrent somatic alterations of FGFR1 and NTRK2 in pilocytic astrocytoma. Nat Genet. 2013; 45:927–932. [PubMed: 23817572]

45. Singh D, Chan JM, Zoppoli P, et al. Transforming fusions of FGFR and TACC genes in human glioblastoma. Science. 2012; 337:1231–1235. [PubMed: 22837387]

46. Natarajan M, Hecker TP, Gladson CL. FAK signaling in anaplastic astrocytoma and glioblastoma tumors. Cancer J. 2003; 9:126–133. [PubMed: 12784878]

47. Yoon CH, Kim MJ, Kim RK, et al. c-Jun N-terminal kinase has a pivotal role in the maintenance of self-renewal and tumorigenicity in glioma stem-like cells. Oncogene. 2012; 31:4655–4666. [PubMed: 22249269]

48. Mendes KN, Wang GK, Fuller GN, Zhang W. JNK mediates insulin-like growth factor binding protein 2/integrin alpha5-dependent glioma cell migration. Int J Oncol. 2010; 37:143–153. [PubMed: 20514406]

49. Versele M, Talloen W, Rockx C, et al. Response prediction to a multitargeted kinase inhibitor in cancer cell lines and xenograft tumors using high-content tyrosine peptide arrays with a kinetic readout. Mol Cancer Ther. 2009; 8:1846–1855. [PubMed: 19584230]

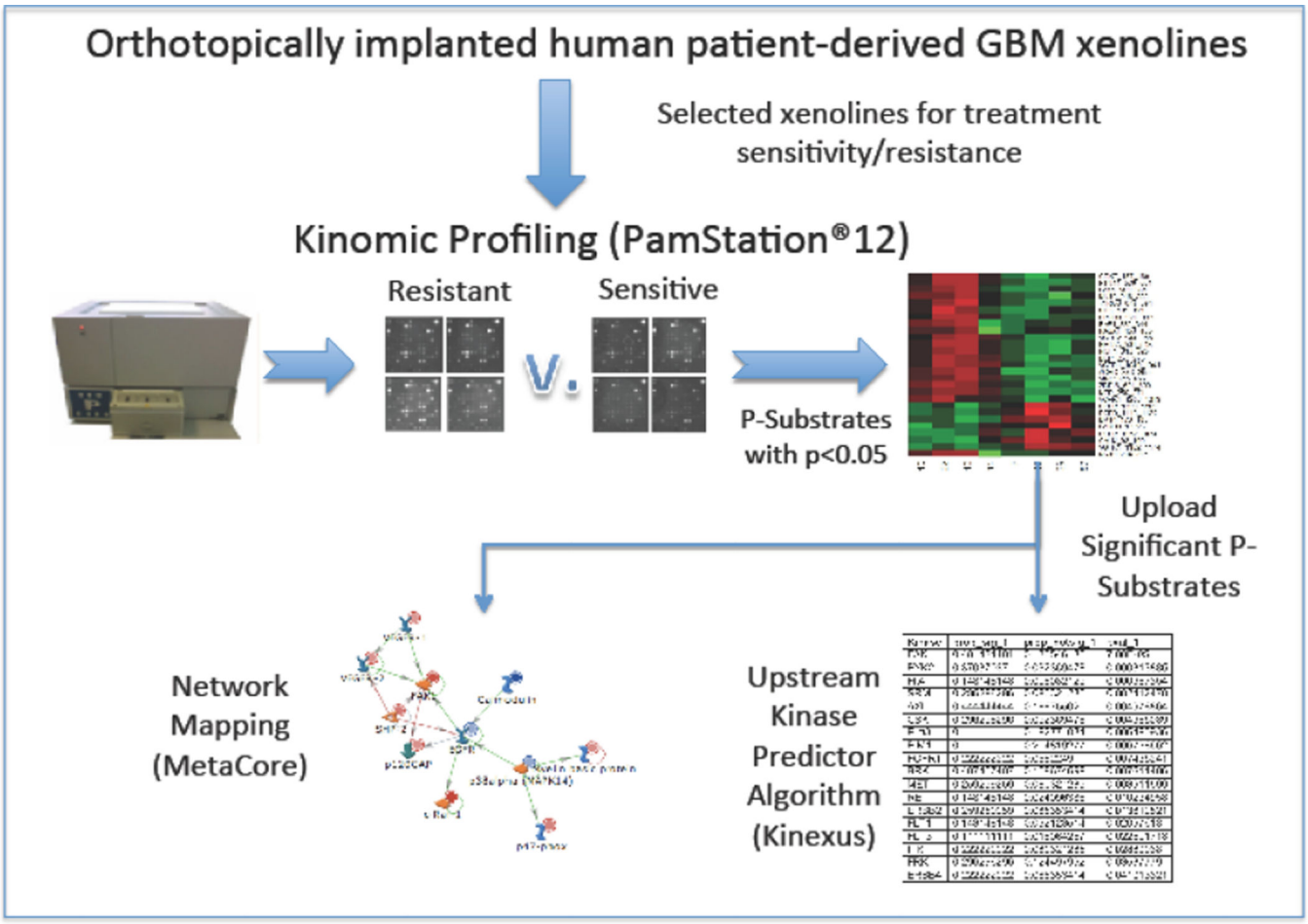

Figure 1.

Schematic of study design and analytical flow. The chip based PamStation®12 platform utilizes a 3D matrix with kinase specific 12–15 amino acid peptides with 1–5 phosphorylatable residues. Lysates are pumped through and phosphorylate residues that are detected using FITC conjugated phosphomotif specific antibodies that are visualized using a CCD camera and analyzed with Evolve and BioNavigator software packages. Treatment sensitive v. resistant tumor kinomic profiles are compared and significant substrates are identified. These are then analyzed for upstream kinase prediction and network mapping.

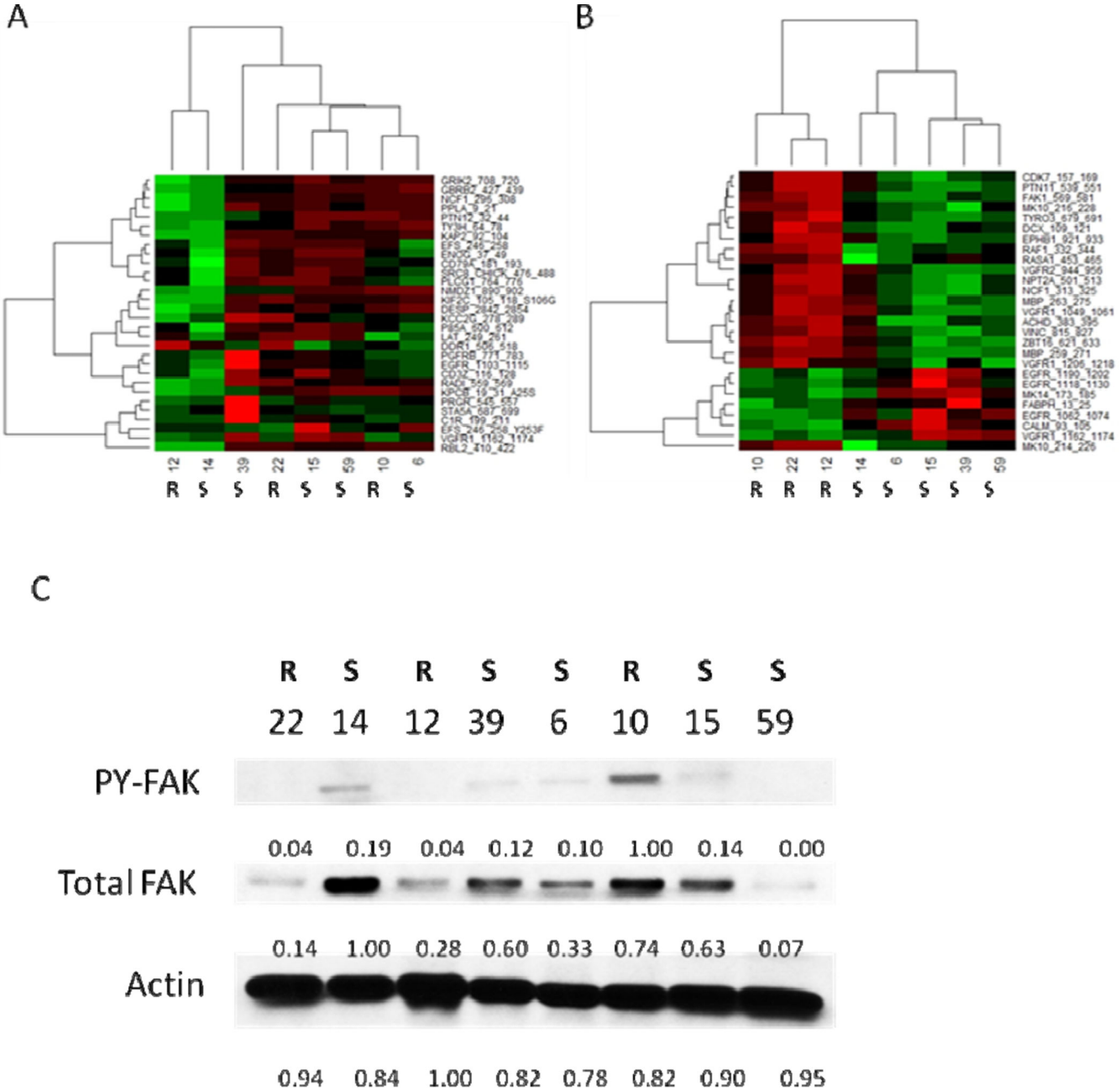

Figure 2.

Kinomic profiling of radiation resistance. Unsupervised hierarchical clustering of variance filtered (var>0.65) kinomic peptide phosphorylation signal (mean of 3 biological replicates) is shown for the 8 tumors with known radiation sensitivity as a heatmap (red indicating decreased signal, and green indicating increased signal) (A). Phosphosubstrates (each peptide is listed as gene name with numbers indicating the amino acids spanning the phosphorylatable substrate, i.e., GRIK2_708_720 is a peptide derived from GRIK2 amino acids 708–720) that were significantly altered in radiation resistant tumors ($p<0.05$ with FDR<0.5) are shown as a hierarchical clustered heatmap (red indicating decreased signal, and green indicating increased signal) (B). Immunoblots of anti-phosphotyrosine 397

(pY397) FAK, total FAK, and actin are shown for each GBM xenoline with densitometry values indicated below the blots (C).

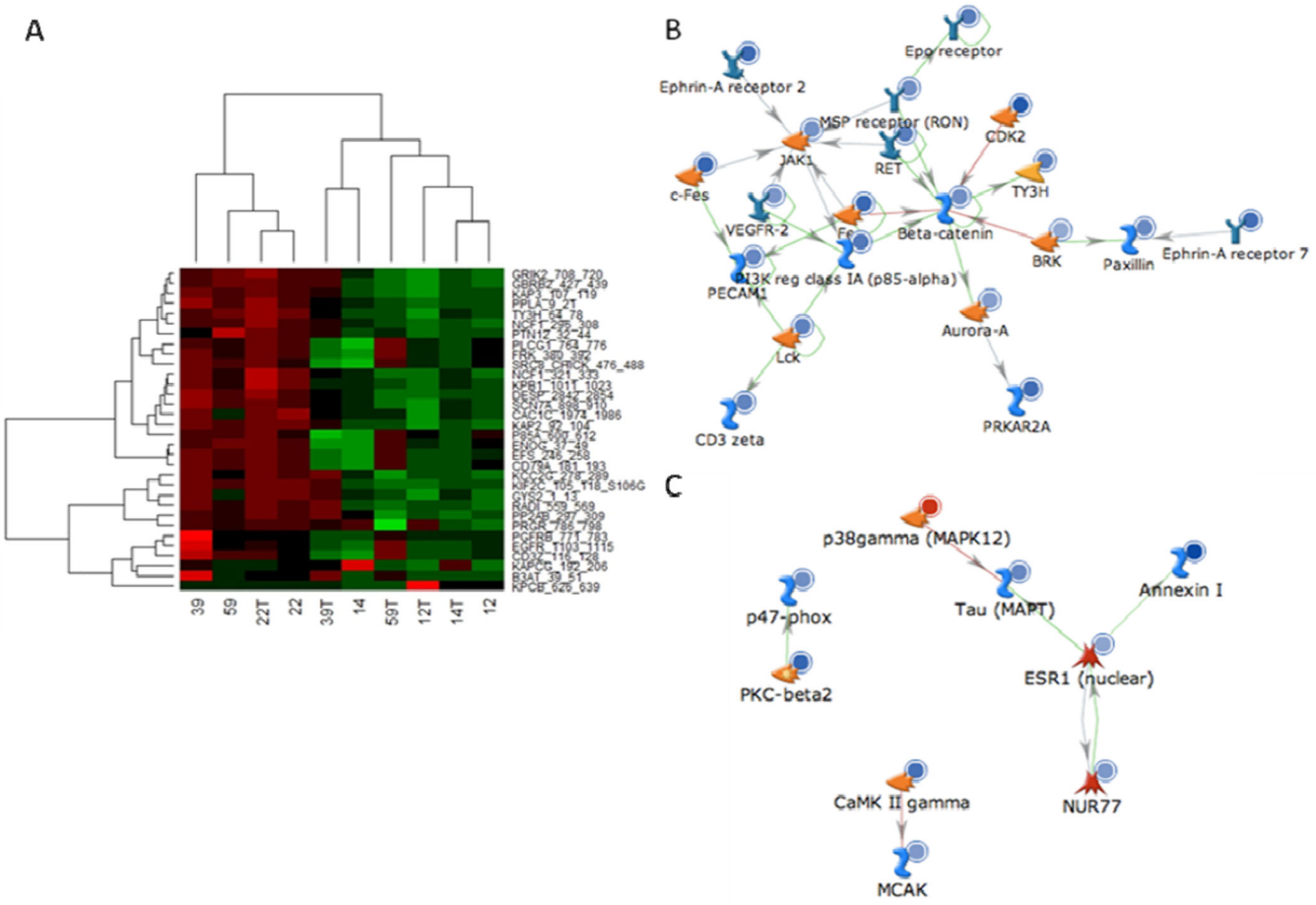

Figure 3.

Kinomic profiling of temozolomide resistance. Unsupervised hierarchical clustering of variance filtered (var>0.75) kinomic peptide phosphorylation signal (mean of 3 biological replicates) is shown for the 5 tumor pairs (parent and TMZ-resistant daughter indicated by "T") as a heatmap (red indicating decreased signal, and green indicating increased signal) (A). Parent gene uniprot ID's of significantly altered peptides ($p<0.05$ and FDR<0.1) in the TMZ resistant GBM39 (B) or GBM59 (C) were mapped to Direct Interactions Networks using MetaCore. Blue circles indicate increased nodes, red circles indicate decreased nodes, green lines indicate positive interactions with red lines indicating negative interactions with direction of interactions annotated with arrows.

Table 1

GBM Xenolines

Orthotopically implanted patient-derived xenografts (xenolines) that were examined including the survival in days of intracranially-implanted parent tumor without TMZ therapy and chronically treated TMZ daughter xenoline tumor receiving TMZ. GBM 6, 10 and 15 tumors did not have TMZ isogenic lines. Radiation sensitivity status (for the parent tumors) and molecular subtypes are indicated based on CLANC algorithm. For GBM ortho 39, two of the 3 biological replicates were of classical molecular subtype while one replicate was of the neural subtype.

Tumor	Survival Parent/TMZ Daughter (in days)	Radiation Sensitivity	Molecular subtype
GBM ortho 12	18/26	Resistant	Classical
GBM ortho 14	27/19	Sensitive	Classical
GBM ortho 22	16/21	Resistant	Mesenchymal
GBM ortho 39	29/25	Sensitive	Classical/Neural
GBM ortho 59	28/27	Sensitive	Mesenchymal
GBM ortho 10	29/ NA	Resistant	Classical
GBM ortho 15	24/ NA	Sensitive	Classical
GBM ortho 6	25/ NA	Sensitive	Classical

Table 2

Upstream Kinase Prediction from Radiation Resistant Tumors.

Kinase	Significant*	Not-Significant**	P value
FAK	48.1%	13.7%	7.00E-05
PYK2	37.0%	9.2%	0.000313885
Flt4	14.8%	0.8%	0.000967354
SRM	29.6%	8.0%	0.002412478
AXL	44.4%	18.9%	0.004978864
CSK	29.6%	9.2%	0.004985089
Pim3	0.0%	19.3%	0.006490936
PIM1	0.0%	20.5%	0.006738662
FGFR1	22.2%	5.6%	0.007435241
BRK	40.7%	16.9%	0.007611406
MET	25.9%	8.0%	0.008911599
RET	14.8%	2.4%	0.010234958
ERBB2	25.9%	8.8%	0.013612821
FLT1	14.8%	3.2%	0.02097613
FLT3	11.1%	1.6%	0.022501718
ITK	22.2%	8.0%	0.02889038
FRK	29.6%	12.4%	0.03537779
ERBB4	22.2%	8.8%	0.041013321

*Proportion of *significant* substrates predicted to be phosphorylated by this kinase

**Proportion of *remaining* substrates predicted to be phosphorylated by this kinase